

Verifying Silicon Photonic Optical Hybrid Designs through Simulation

Benjamin Szamosfalvi

A senior thesis submitted to the faculty of
Brigham Young University
in partial fulfillment of the requirements for the degree of
Bachelor of Science

Ryan Camacho, Advisor

Department of Physics and Astronomy

Brigham Young University

April 14th 2021

Copyright © 2021 Benjamin Szamosfalvi

All Rights Reserved

ABSTRACT

Verifying Silicon Photonic Optical Hybrid Designs through Simulation

Benjamin Szamosfalvi
Department of Physics and Astronomy, BYU
Bachelor of Science

We verify silicon photonic circuit designs for photon number state tomography. We perform homodyne detection using a 90-degree optical hybrid receiver, then reconstruct the input signal's photon number statistics using a maximum likelihood Bayesian estimator. We also demonstrate the potential to reconstruct the photon number statistics of an unknown quantum optical state without single photon detectors or knowledge of the phase of the input states. These devices may be useful for chip-scale quantum information processing tasks in communications, sensing, and computing.

Keywords: silicon photonics, quantum, cryptography, communication, verification, design, tomography

ACKNOWLEDGMENTS

I would like to thank Dr. Ryan Camacho and Brigham Young University for their advice and contribution, and for funding this project. I would also like to thank Christian Carver, Sequoia Ploeg, and Christopher Eyre for their contributions to the project.

Contents

Table of Contents	vii
1 Introduction	1
1.1 Photonics for Quantum Technologies	1
1.2 On-chip Optical Hybrid	3
1.3 Homodyne Detection	5
1.3.1 Ideal Detector with Classical Signal	5
1.3.2 Ideal Detector with Quantum Signal	7
2 Methods	9
2.1 Simulation of Optical Hybrids	9
2.2 Reconstruction of the Input State	13
3 Results and Conclusion	15
3.1 Results	15
3.1.1 Photon Number Reconstructor Results	15
3.1.2 Optical Hybrid Simulation	18
3.2 Conclusion	20
3.3 Future Work	21
Appendix A Quantum Simulation with Strawberry Fields	23
Appendix B Maximum Likelihood Estimator	25
Appendix C Other Code	27
Bibliography	29
List of Figures	29
Index	35

Chapter 1

Introduction

As part of a collaboration with Oak Ridge National Laboratory, we designed an integrated silicon photonic chip for homodyne detection of low-intensity light, and for reconstructing the photon number statistics of an unknown signal. Homodyne detection is the amplification of small electromagnetic waves with a narrow wavelength band by interfering it with a strong signal at the same wavelength, usually called the local oscillator (LO). For this purpose we design, simulate, and verify a 90 degree optical hybrid receiver, then reconstruct the input state using a maximum likelihood estimator (MLE) algorithm.

1.1 Photonics for Quantum Technologies

Optical devices are widely used in modern technology, from laser detection to signal carriers, e.g. fiber optic cables for internet transmission. They have the advantages over regular electronics that they produce less heat, transfer signals faster and with less noise. Another useful property for physicists is that light carrier materials such as fiber glass are inherently less lossy than metal wires and can therefore carry light with very small intensity to be in the quantum regime over distances of up to a few kilometers. Thus, optical devices are prime candidates for performing quantum

optics experiments and building quantum technologies like quantum computers and quantum communication lines.

Silicon photonics are optical devices on the scale of a few hundred microns, like microchips in electronics. Their small size makes silicon photonic devices easily integrable into complex systems like a quantum computer. While free space optics are easier to configure manually, they are not ideal as components of larger systems. Our goal therefore is to design silicon photonic circuits for use in both classical and quantum technologies.

To verify that photonic devices work correctly for quantum experiments, we need to test them using quantum light which introduces extra factors. We will define quantum light here as electromagnetic waves at such low average photon number levels that noise due to quantum uncertainty is greater than noise due to the measurement apparatus. Quantum measurements will exhibit inherently random loss and significant interference effects can appear which are not present in classical measurements, making it difficult to prove our designs' correctness. Therefore, we simulate the ideal version of our devices in both the classical and quantum regimes to find faults in their designs before sending them to fabrication. This lowers fabrication costs and waiting times due to finding mistakes in designs after laboratory testing and having to manufacture a new set of devices each time.

Taking data for determining classical properties of silicon photonic devices is straightforward, but the measurement difficulties when using quantum light make it hard to test photonic devices for quantum experiments since we cannot measure the signal inside the device like with free space optical setups. We can minimize the amount of uncertainty by measuring the loss of non-integrated optical components like our off-chip beam splitters and fiber cables, and by measuring the signal intensity before and after several calibration devices on-chip to identify grating coupler and waveguide losses (Figure 1.1).

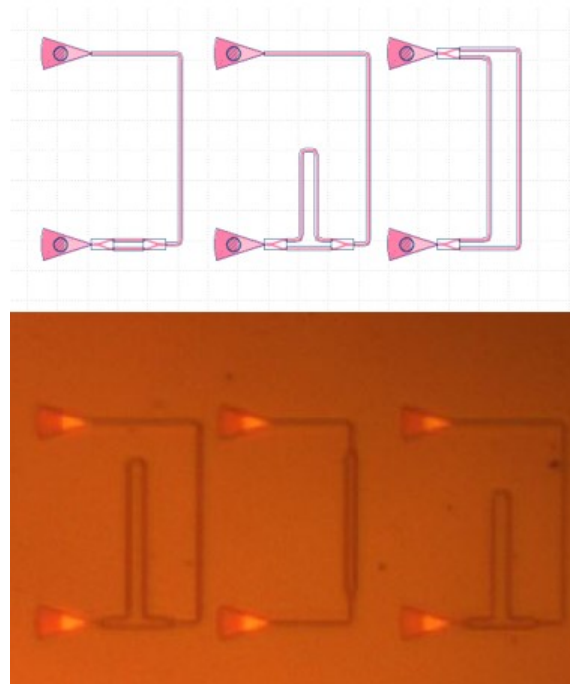


Figure 1.1 Mach-Zehnder interferometers used for measuring waveguide and grating coupler losses as a function of wavelength. Design in KLayout (above) and fabricated devices (below).

1.2 On-chip Optical Hybrid

As a specific example, we simulate a 90° optical hybrid. The purpose of this device is to interfere two signals and output their linear combination, with one signal's phase varying by $\frac{\pi}{2}$ between 4 outputs.

Our initial designs for the optical hybrids are made up of a core with two Y-branches to split the two inputs, two 50-50 directional couplers which serve as beam splitters, and grating couplers for the interface between the chip and off-chip.

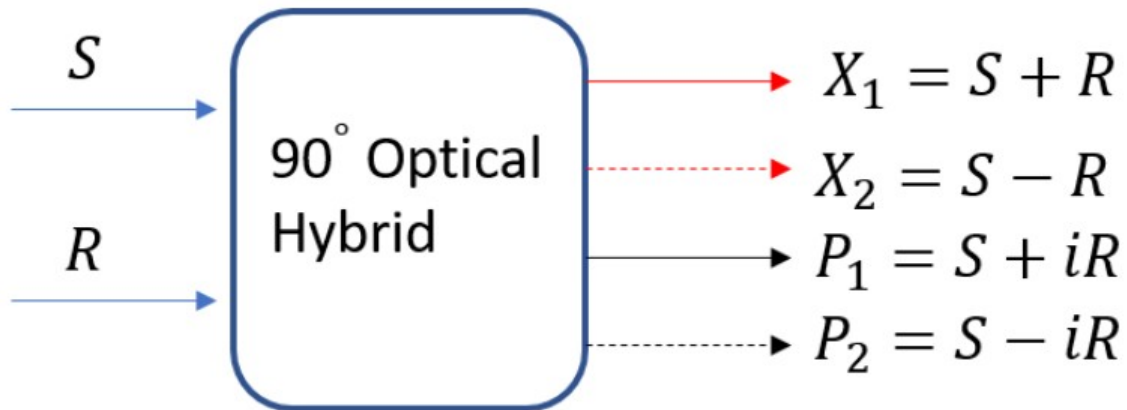


Figure 1.2 High-level operation of a 90° optical hybrid, with the two inputs being the unknown signal (S) and the reference field (R), the latter also known as the local oscillator.

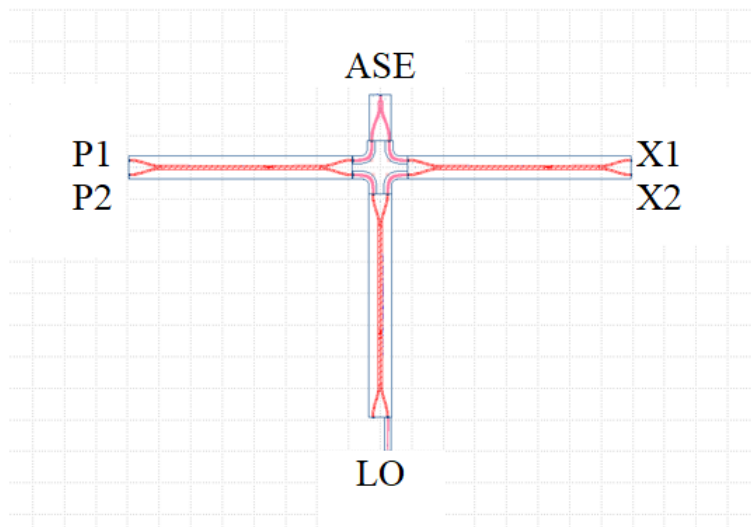


Figure 1.3 Layout of the optical hybrid core in the design software KLayout. The signal input is labeled as ASE (Amplified Spontaneous Emission) which usually stands for thermal light, but for the purposes of this paper the input signal can be any quantum light state. The bottom input is the Local Oscillator (LO) and the four outputs X_1 , X_2 , P_1 , P_2 are given as shown in 1.2

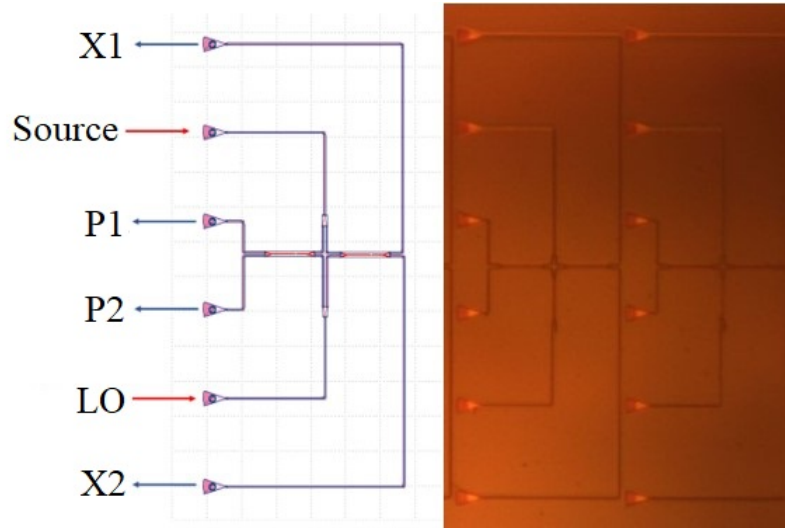


Figure 1.4 Layouts and microscope pictures of fabricated optical hybrids showing input and output grating coupler ports.

1.3 Homodyne Detection

We will use the optical hybrids for homodyne detection, which means interfering two signals with the same wavelength to measure the weaker one while filtering out noise at different frequencies using the orthogonality property of sine waves over integration times much larger than the signal's oscillation period.

1.3.1 Ideal Detector with Classical Signal

First we will describe the operation of an optical hybrid for classical operation. We first write our input signal and reference fields as a vector:

$$E_{in} = \begin{bmatrix} E_s \\ E_r \end{bmatrix} \quad (1.1)$$

The 90° optical hybrid takes in two input fields and produces four output fields according to the following transfer matrix:

$$H = \frac{1}{2} \begin{bmatrix} 1 & 1 \\ 1 & -1 \\ 1 & i \\ 1 & -i \end{bmatrix} \quad (1.2)$$

After passing through the optical circuit, the resulting 4 output fields are:

$$E_{out} = \frac{1}{2} \begin{bmatrix} 1 & 1 \\ 1 & -1 \\ 1 & i \\ 1 & -i \end{bmatrix} \begin{bmatrix} A_s e^{i\theta_s} \\ A_r e^{i\theta_r} \end{bmatrix} = \frac{1}{2} \begin{bmatrix} A_s e^{i\theta_s} + A_r e^{i\theta_r} \\ A_s e^{i\theta_s} - A_r e^{i\theta_r} \\ A_s e^{i\theta_s} + iA_r e^{i\theta_r} \\ A_s e^{i\theta_s} - iA_r e^{i\theta_r} \end{bmatrix} \quad (1.3)$$

If we place each field on a photodetector we obtain 4 electronic signals with amplitudes proportional to $|E_{out}|^2$:

$$|E_{out}|^2 = \frac{1}{4} \begin{bmatrix} A_s^2 + A_r^2 + 2A_s A_r \cos(\theta_r - \theta_s) \\ A_s^2 + A_r^2 - 2A_s A_r \cos(\theta_r - \theta_s) \\ A_s^2 + A_r^2 + 2A_s A_r \sin(\theta_r - \theta_s) \\ A_s^2 + A_r^2 - 2A_s A_r \sin(\theta_r - \theta_s) \end{bmatrix} \equiv \begin{bmatrix} X_1 \\ X_2 \\ P_1 \\ P_2 \end{bmatrix} \quad (1.4)$$

Now we have defined X_1, X_2, P_1 , and P_2 . We further define new quantities X and P as

$$X \equiv X_1 - X_2 = A_s A_r \cos(\theta_r - \theta_s) \quad (1.5)$$

$$P \equiv P_1 - P_2 = A_s A_r \sin(\theta_r - \theta_s) \quad (1.6)$$

Since we know the values of the reference amplitude and phase, we can solve for the values of the signal amplitude and phase:

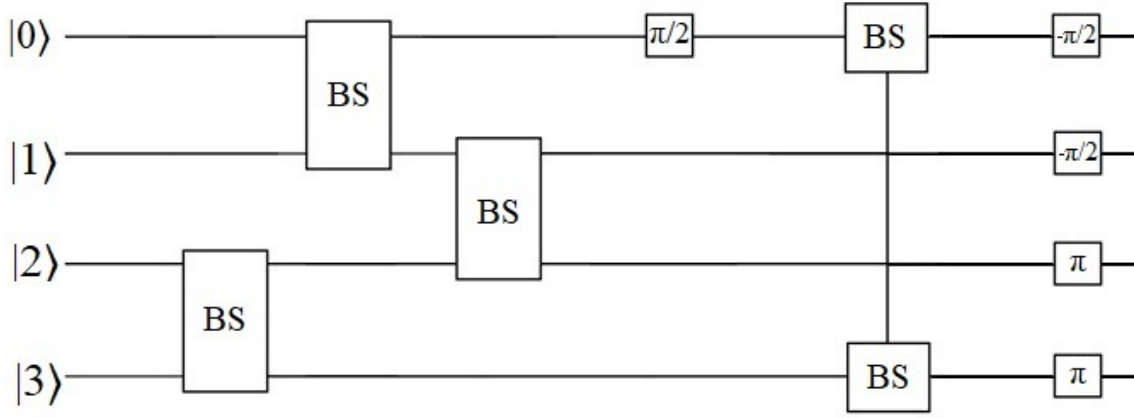


Figure 1.5 Line circuit model of an ideal 90° optical hybrid.

$$A_s = \frac{\sqrt{X^2 + P^2}}{A_r} \quad (1.7)$$

$$\theta_s = \theta_r - \arctan\left(\frac{P}{X}\right) \quad (1.8)$$

1.3.2 Ideal Detector with Quantum Signal

The circuit diagram Figure 1.5 shows the operators we must apply on the input states to achieve the desired effect of an optical hybrid. The multiples of π are rotation gates, and **BS** are 50-50, symmetric beam splitters whose effect can be written as $\mathbf{BS}_{12} = \exp\left[\frac{i\pi}{4}(\hat{a}_1\hat{a}_2^\dagger + \hat{a}_1^\dagger\hat{a}_2)\right]$. We will derive the effect of the above optical hybrid acting on an input state for the case of coherent states. Start by using 4 arbitrary coherent states as input.

$$|\psi\rangle = |\alpha\rangle_0 |\beta\rangle_1 |\gamma\rangle_2 |\xi\rangle_3 \quad (1.9)$$

Apply the first set of beam splitters, and then the rotation gate,

$$|\psi'\rangle = \mathbf{BS}_{01}\mathbf{BS}_{23}|\psi\rangle = \left|\frac{\alpha+i\beta}{\sqrt{2}}\right\rangle_0 \left|\frac{i\alpha+\beta}{\sqrt{2}}\right\rangle_1 \left|\frac{\gamma+i\xi}{\sqrt{2}}\right\rangle_2 \left|\frac{i\gamma+\xi}{\sqrt{2}}\right\rangle_3 \quad (1.10)$$

$$|\psi'_R\rangle = \mathbf{R}_0^{\frac{\pi}{2}} |\psi'\rangle = \left| \frac{i\alpha - \beta}{\sqrt{2}} \right\rangle_0 |\dots\rangle_{1-3} \quad (1.11)$$

Then apply the second set of beam splitters

$$|\psi''\rangle = \mathbf{BS}_{03} \mathbf{BS}_{12} |\psi'_R\rangle = \left| \frac{i\alpha - \beta - \gamma + i\xi}{2} \right\rangle_0 \left| \frac{i\alpha + \beta + i\gamma - \xi}{2} \right\rangle_1 \left| \frac{-\alpha + i\beta + \gamma + i\xi}{2} \right\rangle_2 \left| \frac{-\alpha - i\beta + i\gamma + \xi}{2} \right\rangle_3 \quad (1.12)$$

To match our experiment, we will set $\beta = \gamma = 0$ to get

$$|\psi''\rangle(\alpha, 0, 0, \xi) = \left| \frac{i\alpha + i\gamma}{2} \right\rangle_0 \left| \frac{i\alpha - \gamma}{2} \right\rangle_1 \left| \frac{-\alpha + i\gamma}{2} \right\rangle_2 \left| \frac{-\alpha + \gamma}{2} \right\rangle_3 \quad (1.13)$$

Finally, we apply the rotation gates to get the final result

$$\mathbf{R}_{0,1}^{-\frac{\pi}{2}} \mathbf{R}_{2,3}^{\pi} |\psi''\rangle = \left| \frac{\alpha + \gamma}{2} \right\rangle_0 \left| \frac{\alpha + i\gamma}{2} \right\rangle_1 \left| \frac{\alpha - i\gamma}{2} \right\rangle_2 \left| \frac{\alpha - \gamma}{2} \right\rangle_3 \quad (1.14)$$

If we take input mode 0 to be the Source and mode 3 to be the LO, then the resulting states exactly correspond to the four quadratures we introduced in 1.2. This shows that the circuit model we designed does represent a 90° optical hybrid, as desired.

The theory for homodyne detection is straightforward, as described above. However, to be able to simulate the effect of the above circuit, we have to convert the discrete Fock basis states into continuous functions in electromagnetic phase space, called Wigner functions. This lets us work with the quantum state as a function whose domain is in \mathbb{R}^2 , making numerical calculation much faster. Note that unlike a classical system which is a point in phase space, quantum light is a distribution over two-dimensions.

Chapter 2

Methods

2.1 Simulation of Optical Hybrids

To determine whether our designed optical hybrids will perform nominally, we simulate an ideal optical hybrid's behavior when using quantum inputs. For this method, we assume that the optical hybrids produce an exact 90° phase shift between the output. We have shown using classical simulations and by measuring the fabricated devices that the correct phase shifts can be achieved at one wavelength point in the 1550–1620 nm range. Note that this point varies between each individual device due to potential differing jog lengths and manufacturing variance.

We use the python package Strawberry Fields [1], an open-source photonic circuit simulation library, to simulate an ideal 90° optical hybrid. We use the following process to model our circuit:

1. Initialize the modes $|0\rangle$ and $|3\rangle$ to be the unknown source and the local oscillator.
2. Rotate the source mode by $\frac{\pi}{2}$.
3. Split the input modes evenly between 0 and 1, and 2 and 3.
4. Interfere the signals between modes 1 and 2, and 0 and 3 using 50-50 beam splitters.

5. Rotate the outputs so the LO term is at a 90° relative phase relative between the output modes.

This should lead to a 90 degree phase shift between the 4 outputs. Figure 1.5 shows the device using an optical circuit model and Appendix A shows the code used to simulate the device.

The two options for backends for the simulation engine are 'gaussian' and 'fock'. The Fock backend uses the number state basis of a quantum harmonic oscillator and performs the computations using matrix multiplications, while the Gaussian backend operates by converting the quantum states into a phase-space representation in quadrature phase space. The quadrature operators we use are

$$\hat{X} = \frac{1}{\sqrt{2}}(\hat{a}^\dagger + \hat{a}) \quad \hat{P} = \frac{1}{\sqrt{2}}(\hat{a}^\dagger - \hat{a}) \quad (2.1)$$

and the phase space representation of a quantum state is a continuous function $\psi(x, p)$ whose values are proportional to the probability amplitude of the state at each (x, p) coordinate. For illustration purposes, we will use the Wigner function as our phase-space function of choice.

As explained at the end of Section 1.3.2, the Gaussian backend offers significant speedup and scaling for larger photon numbers over the Fock backend. In exchange, if we want to obtain information about the state in the Fock basis, we must convert the output state to the Fock basis using a reverse Wigner-Weyl transform.

The simulation results can be interpreted on an intuitive level by plotting the Wigner functions of the output state in phase space. We illustrate the four outputs on the same plot for convenience. The states starting at angle 0 and going counterclockwise are in order As Figures 2.1–2.3 illustrate, the LO magnitude is proportional to the states' distance from the origin radially and the states are displaced by the vector corresponding to the source's complex number α . As expected, coherent states in phase space are represented by circular regions with minimum uncertainty.

Using a thermal state for the input signal eliminates any phase information, and its effect is to widen the state's phase space representation around the LO's locations. Figure 2.4 shows this effect as a function of the input thermal state's average photon number.

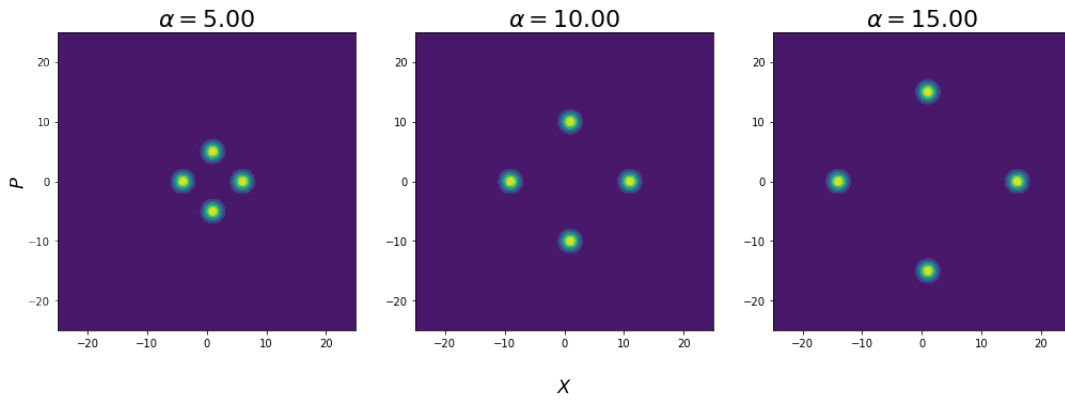


Figure 2.1 Strawberry Fields simulation of the optical hybrid outputs. The input signal and local oscillator are both Coherent signals. The input signal’s magnitude is set to $\alpha_{Source} = 1$ and the LO magnitude is varied (corresponding complex number displayed above plots).

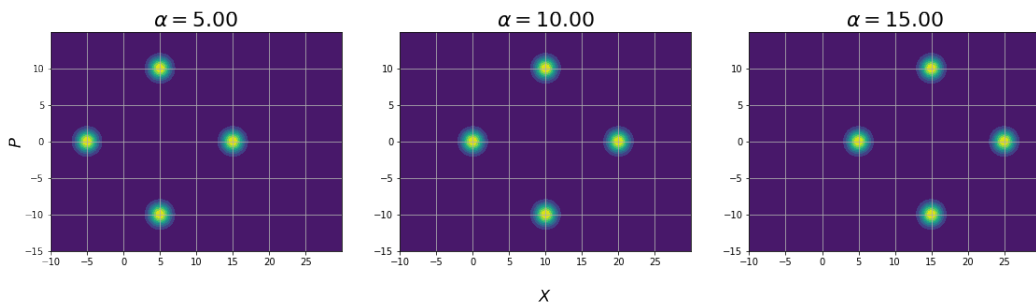


Figure 2.2 We set the LO magnitude to be constant, and increase the signal magnitude (corresponding complex number displayed above plots).

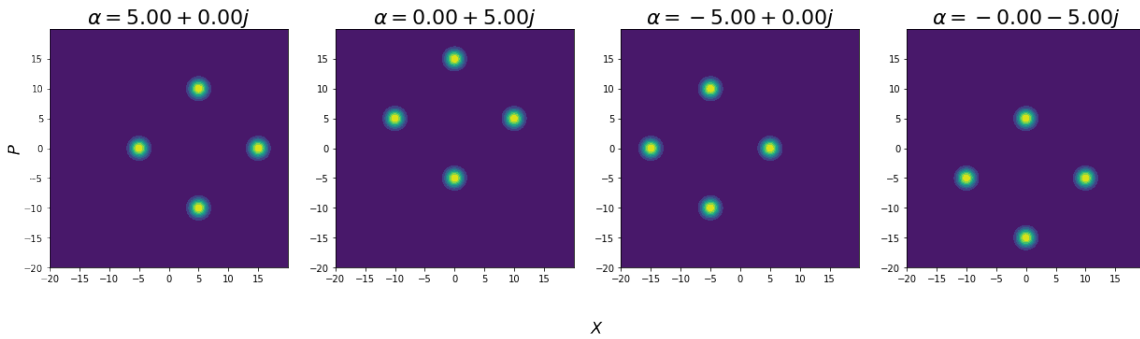


Figure 2.3 We set the LO and source magnitudes to be constant, and vary the source’s phase (corresponding complex number displayed above plots).

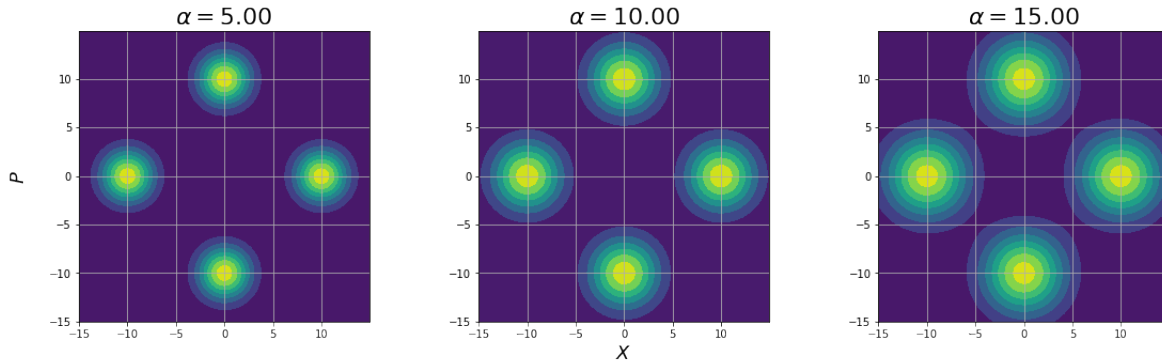


Figure 2.4 The output of the optical hybrid plotted in phase space as Wigner functions with a coherent state Local Oscillator with $\alpha = 10$, and thermal state Input Signals at $\alpha = 5, 10, 15$.

We can use one of two methods to find quadrature measurement statistics from Wigner functions:

1. Use Strawberry Fields' builtin function `BaseGaussianState.all_fock_probs()` for retrieving all number state probabilities up to a certain photon number cutoff. This computationally intensive, and is impractical to perform past total photon numbers of 60 due to memory restrictions. However, it is possible to get each basis state's probability separately, and then perform post-selection to store the large probability values using `fock_prob()` function. This mitigates the computational cost somewhat.
2. Assume that the number state distribution for each mode is proportional to some known distribution, e.g. Bose-Einstein or Poisson. Retrieve the mean and covariance of the states using `reduced_gaussian()`, then use the ideal distribution formula with these parameters.

We can compile the statistics obtained using one of these methods into distributions that we can then sample to get our simulated measurement points. Once we have the measurement points, we calculate Z for each point according to

$$Z = \frac{\sqrt{(X_1 - X_2)^2 + (P_1 - P_2)^2}}{|\alpha_{ref}|} \quad (2.2)$$

where the quadrature values correspond to the modes

$$|0\rangle = X_1, \quad |1\rangle = P_1, \quad |2\rangle = P_2, \quad |3\rangle = X_2. \quad (2.3)$$

The resulting Z points can then be fed into the MLE algorithm to retrieve the predicted input state. However, we first construct a histogram from the Z points by binning the values over a discrete grid, then we compare the resulting distribution to the ideal Z distribution function

$$P_Z(z) = e^{-z} \sum_{n=0}^{\infty} \frac{\rho_{nn}}{n!} z^n. \quad (2.4)$$

derived by Qi, Lougovski, and Williams [2], where ρ_{nn} represents the input state's density matrix's diagonal elements. If the two distributions match closely, we can know that the ideal optical hybrid simulation works correctly.

2.2 Reconstruction of the Input State

The probability distribution of the number states in the input signal must be determined using statistical methods since the measurements only tell us the photon number measured in one shot measurement. Further, since we are not using single photon detectors, we cannot bin the results directly as the Z points will not resemble the underlying photon number distribution. Thus, we turn to a Bayesian maximum likelihood estimator (MLE) algorithm designed by Qi, Lougovski, and Williams [2], and implemented by us.

The MLE method returns a photon number probability distribution given the input data. We then compare the resulting distribution to the probability distribution of the input signal using least squares error. If the reconstructed distribution matches the original well (to within 1.0%), then the designs meet the requirements.

Chapter 3

Results and Conclusion

3.1 Results

3.1.1 Photon Number Reconstructor Results

First, we ran tests to verify our Maximum Likelihood Estimator algorithm. Verifying the reconstructor first lets us use it to verify the optical hybrid simulation later, knowing that our reconstructor works correctly.

We used ideal coherent and thermal light state data which correspond to Poisson and Bose-Einstein number state distributions. We varied the average photon number for the input states between $\bar{n} = 1$ to 20 as shown in Figure 3.1. For coherent states we let the estimator run up to 10 iterations, for thermal states up to 5 iterations maximum (Figure 3.2). We set our cutoff photon number in the simulations to be $\max(3\bar{n}, 10)$ to make sure all number states with large probability percentage would be included in the domain.

We use the root mean squared error as the metric to evaluate our reconstructor's correctness. Figure 3.3 shows the error as a function of average photon number for the both input distribution types. The error spikes for low average photon numbers, but the two quantities seem to be inversely

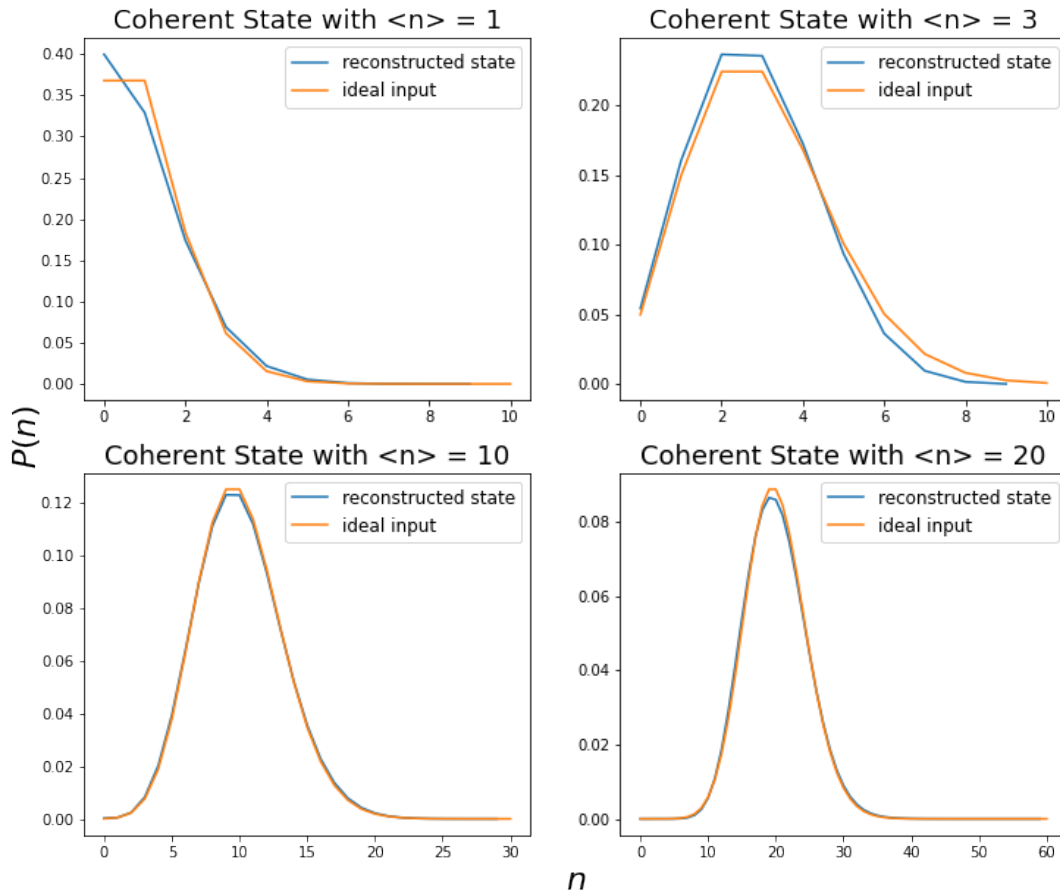


Figure 3.1 Comparison of photon number reconstruction results with the input coherent state.

proportional in general. Notably, the coherent state error goes up to 10%, while the thermal state error is less than 0.2%.

The low error percentages show that our reconstructor is working nominally when used with the right parameters, therefore we can use it with confidence to reconstruct the photon number statistics of our simulated devices.

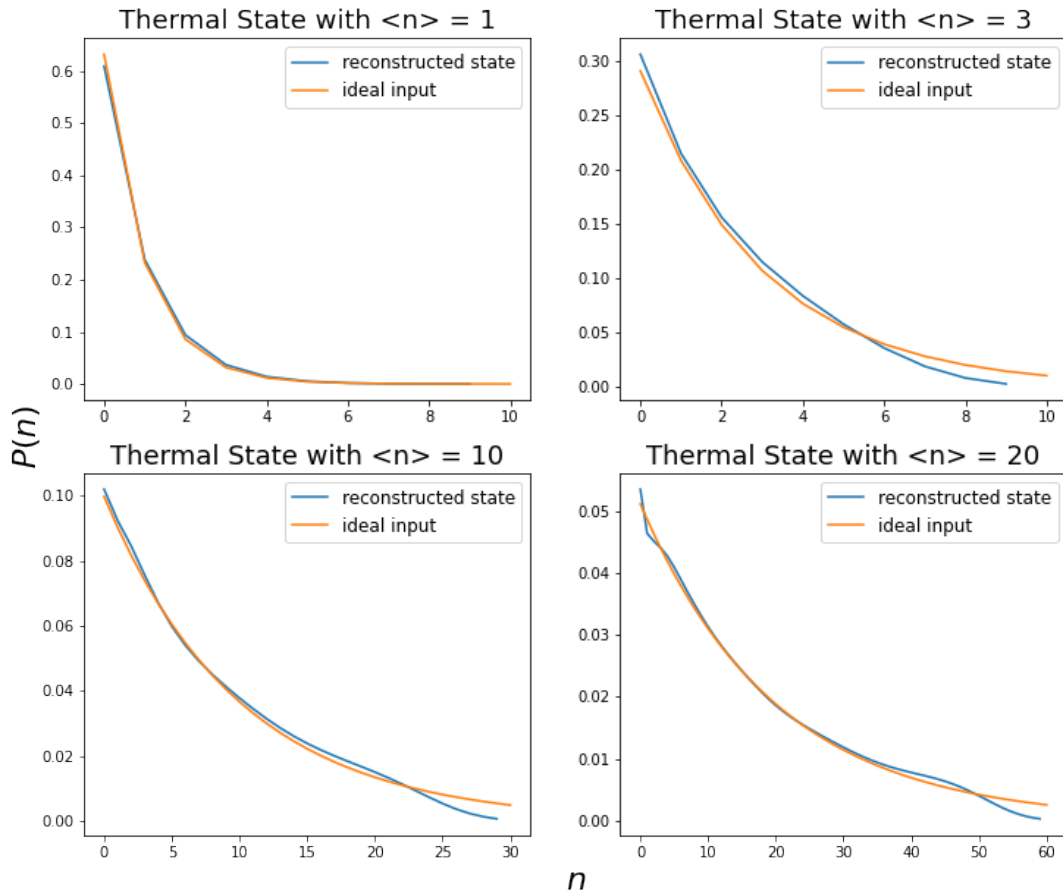


Figure 3.2 Reconstruction comparison with thermal states, using units where $kT = \langle n \rangle$.

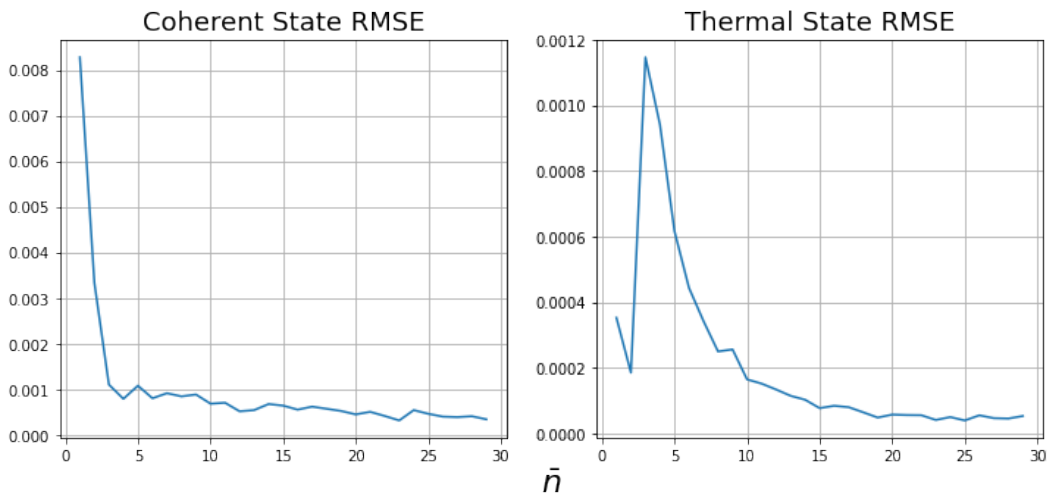


Figure 3.3 Root mean squared error of the probability values between the reconstructed and original states. The error ratio is calculated by running the reconstructor for each average photon number, calculating the total RMSE, and dividing it by the mean value of the input distribution.

3.1.2 Optical Hybrid Simulation

Next, we proceeded to run the Strawberry Fields simulation for the optical hybrid. After post-selecting the high probability states and constructing a probability distribution of the remaining basis Fock states, we sampled the resulting distribution to acquire Z measurement points. Finally, we constructed a histogram from the Z points by binning them.

The strawberry fields simulations we could carry out were somewhat limited due to memory limitations. We used Google Colaboratory notebooks which have roughly 12 GB of memory, which allows simulating up to about 60–70 total photons in the system since the number of basis states grows like $O(n!)$ as a function of maximum considered photon number. Therefore we had to use a LO with average photon number of about 50, while an ideal LO would have intensity that is orders of magnitude larger than the source intensity.

We simulated the ideal optical hybrids with coherent states as both the "unknown" signal and the local oscillator, as shown in Figure 3.4.

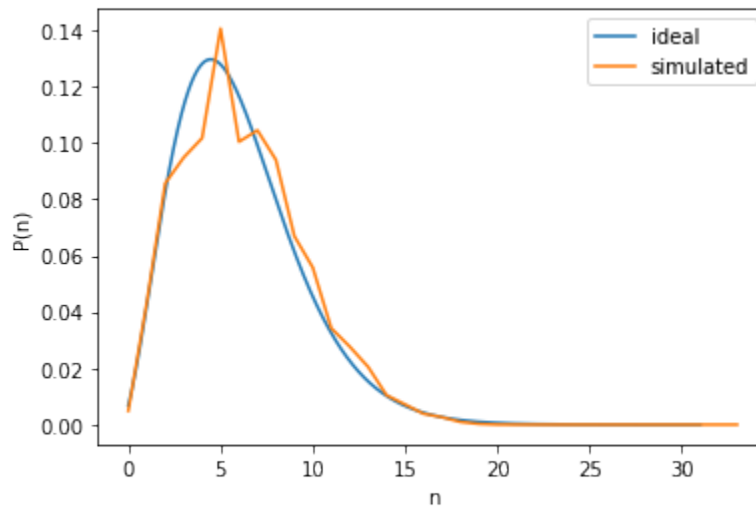


Figure 3.4 Simulated Z measurements using a signal with average photon number $\langle n \rangle = 5$ compiled into a histogram (simulated). [2]

The resulting distribution matches the ideal Z distribution relatively well for this specific photon

number. We then apply the MLE algorithm to the given data, giving us the reconstructed photon number distribution in Figure 3.5.

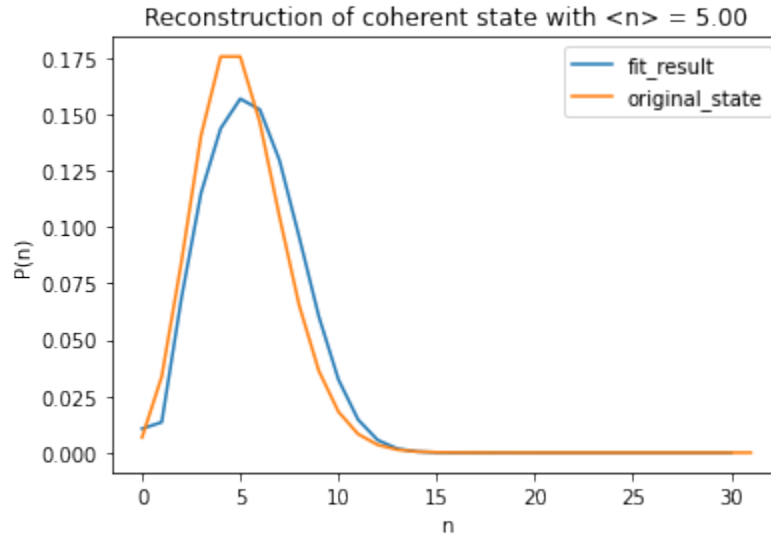


Figure 3.5 Reconstructed photon number distribution (blue) and the original state (orange).

Again, the resulting distribution matches the original state relatively well.

We ran a few more simulations with different average photon numbers, and found that the resulting Z data does not match the ideal Z distribution well. Figure 3.6 shows the major issue we came across. Changing the magnitude of the LO proportionally changed the predicted output, which is not desirable, as it prevents us from getting independent information about the unknown source.

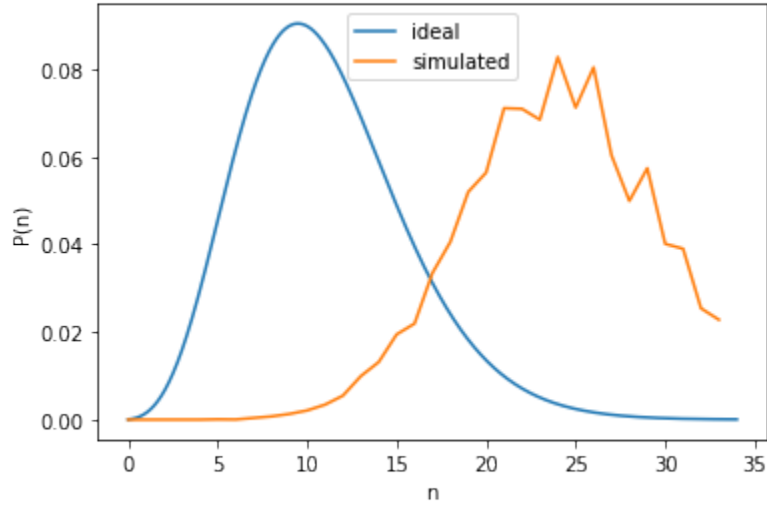


Figure 3.6 Ideal Coherent number state probabilities compared with the reconstructed state. The reconstructed state predicts an average photon number that is larger than the original number.

3.2 Conclusion

We designed an ideal circuit/operator model for a 90° optical hybrid receiver, and wrote code to simulate the device in Strawberry Fields, post-process the data, and finally use a Maximum Likelihood Estimator algorithm to reconstruct the number state distribution of the input state. We demonstrated the correctness of the MLE algorithm, but we encountered issues with the simulation of the device.

We suspect that the error in the predictions is caused by incorrect post-processing, specifically we are calculating the Z data from the photon number sampling measurements in a way that doesn't completely remove the dependence on the LO's magnitude from the final measurement results. Another reason could be that the LO intensities we used were too small, so we did not meet the requirements for using the optical hybrid for photon number tomography.

Once these issues are solved, we can extend the same procedure to simulate and verify other inte-

grated photonic circuit designs for future research. This process will produce evidence supporting the correctness of our designs quickly and conveniently. Additionally, the verification process will eliminate potential design mistakes before fabrication, saving up to several thousands of dollars in fabrication costs.

3.3 Future Work

We are still waiting for experimental measurements from the fabricated optical hybrids. Our planned next step is to compare Z measurements from a physical chip to find further evidence to support our optical hybrid designs.

Once the ideal device simulations are nominal, we could introduce losses and interference in the optical components of the device by decorating the built-in Strawberry Fields loss operators to allow custom losses. We would then probabilistically apply loss and phase shift operators to simulate the effects of waveguide loss and path length variations due to manufacturing. Finally, we would record the effects of these losses on the reconstructed distributions and later use them to remove the effect of experimental variation from measurements on the physical chips. This addition could warn the designers of potential issues that would need to be addressed either by changing the ideal design or the physical chip layout before fabrication.

The simulation software could also be integrated with Symphony, an open-source classical photonic circuit simulation library written by Ploeg, Gunther, and Camacho [3]. A layout written in python source code could be compiled into a Strawberry Fields circuit programmatically to speed up the design process, and perhaps even allow designers without a quantum optics background to verify designs for quantum processes.

Appendix A

Quantum Simulation with Strawberry Fields

```
1 import strawberryfields as sf
2 from strawberryfields.ops import *
3
4 def simulate_optical_hybrid(signal, reference, input_state=Coherent):
5
6     eng = sf.Engine(backend="gaussian")
7     prog = sf.Program(4)
8     with prog.context as q:
9         input_state(np.abs(signal), np.angle(signal)) | q[0]
10        Coherent(np.abs(reference), np.angle(reference)) | q[3]
11        BSGate(np.pi/4, np.pi/2) | (q[0], q[1])
12        BSGate(np.pi/4, np.pi/2) | (q[2], q[3])
13        Rgate(np.pi/2) | q[0]
14        BSGate(np.pi/4, np.pi/2) | (q[1], q[2])
15        BSGate(np.pi/4, np.pi/2) | (q[0], q[3])
16        Rgate(-np.pi/2) | q[0]
```

```
17     Rgate(-np.pi/2)         | q[1]
18     Rgate(np.pi)           | q[2]
19     Rgate(np.pi)           | q[3]
20
21     return eng.run(prog).state
```

Listing A.1 Strawberry Fields code for simulating the ideal optical hybrid.

Appendix B

Maximum Likelihood Estimator

```
1 import numpy as np
2 from scipy.special import factorial
3 from scipy.stats import poisson
4
5
6 class ExpMax:
7     def __init__(self, n_states, max_iter=100, tol=1e-5, verbose=False):
8         self.n_states = n_states
9         self.max_iter = max_iter
10        self.tol = tol
11        self.verbose = verbose
12
13    def fit(self, X, prior=None, lam=5):
14        M = len(X)
15
16        # Initialize the photon number probability distribution array
17        theta.
18
19        if prior == "UNIFORM" or prior is None:
20            theta = np.ones(self.n_states) / self.n_states
```

```

19     elif prior == "POISSON":
20         theta = poisson.pmf(np.arange(self.n_states), lam)
21
22         # Calculate the Z-distribution for each of several measurement
23         # points X.
24         p_z = lambda n, z: np.exp(-z)*z**n / factorial(n)
25         z_prob = np.array([p_z(np.arange(self.n_states), z) for z in X])
26
27         # Perform Maximum Likelihood Estimation iteration
28         for m in range(self.max_iter):
29             theta_old = theta.copy()
30             q = theta * z_prob
31             q_temp = q.copy() # save for use in printing likelihood
32             q = q / np.sum(q, axis=1).reshape(-1,1)
33             # Sum the rows, renormalize.
34             theta = np.sum(q, axis=0) / M
35             if self.verbose:
36                 print(m, np.linalg.norm(theta-theta_old),
37                       np.sum(np.log(np.sum(q_temp, axis=1))))
38
39             # If the probability values don't change within tolerance,
40             # stop iterating.
41             if np.linalg.norm(theta-theta_old) < self.tol:
42                 break
43
44         self.coeffs = theta
45         return theta

```

Listing B.1 Maximum Likelihood Estimator algorithm for reconstructing photon number statistics.

Appendix C

Other Code

```
1 inputs = [np.sqrt(2), np.sqrt(10), np.sqrt(20)]
2 ref = np.sqrt(40)
3
4 # input_state = Coherent(np.abs(signal), np.angle(signal))
5 input_states = [Thermal(np.abs(input)) for input in inputs]
6 states = [simulate_optical_hybrid(input, ref) for input in input_states]
7
8 x_grid = np.arange(-9, 9, 0.01)
9 p_grid = np.arange(-9, 9, 0.01)
10 combined_wigners = [state.wigner(0, x_grid, p_grid) + state.wigner(1,
    x_grid, p_grid) + state.wigner(2, x_grid, p_grid) + state.wigner(3,
    x_grid, p_grid) for state in states]
11
12 fig = plt.figure(figsize=(17,5))
13 ax = fig.add_subplot(111)
14 ax.spines['top'].set_color('none')
15 ax.spines['bottom'].set_color('none')
16 ax.spines['left'].set_color('none')
17 ax.spines['right'].set_color('none')
```

```
18 ax.tick_params(labelcolor='w', top=False, bottom=False, left=False,
    right=False)
19 ax.set_xlabel('$X$', fontsize=14)
20 ax.set_ylabel('$P$', fontsize=14)
21
22 for i, combined_wigner in enumerate(combined_wigners):
23     ax_i = fig.add_subplot(1, len(combined_wigners), i + 1)
24     ax_i.contourf(x_grid, p_grid, combined_wigner)
25     ax_i.set_aspect('equal')
26     ax_i.set_title('$\\bar{{n}} = {0:.2f}$'.format(inputs[i]**2))
27 fig.show()
```

Listing C.1 Plotting code for illustrating the outputs of the Strawberry Fields simulations in phase space using Wigner functions.

Bibliography

- [1] Xanadu, “Strawberry Fields,” (Accessed February 10, 2021).
- [2] B. Qi, P. Lougovski, and B. P. Williams, “Characterizing photon number statistics using conjugate optical homodyne detection,” *Optics Express* **28**, 2276–2290 (2020).
- [3] CamachoLab, “Symphony,” (Accessed March 10, 2021).

List of Figures

1.1	Mach-Zehnder interferometers used for measuring waveguide and grating coupler losses as a function of wavelength. Design in KLayout (above) and fabricated devices (below).	3
1.2	High-level operation of a 90° optical hybrid, with the two inputs being the unknown signal (S) and the reference field (R), the latter also known as the local oscillator. .	4
1.3	Layout of the optical hybrid core in the design software KLayout. The signal input is labeled as ASE (Amplified Spontaneous Emission) which usually stands for thermal light, but for the purposes of this paper the input signal can be any quantum light state. The bottom input is the Local Oscillator (LO) and the four outputs X1, X2, P1, P2 are given as shown in 1.2	4
1.4	Layouts and microscope pictures of fabricated optical hybrids showing input and output grating coupler ports.	5
1.5	Line circuit model of an ideal 90° optical hybrid.	7
2.1	Strawberry Fields simulation of the optical hybrid outputs. The input signal and local oscillator are both Coherent signals. The input signal's magnitude is set to $\alpha_{Source} = 1$ and the LO magnitude is varied (corresponding complex number displayed above plots).	11

2.2	We set the LO magnitude to be constant, and increase the signal magnitude (corresponding complex number displayed above plots).	11
2.3	We set the LO and source magnitudes to be constant, and vary the source's phase (corresponding complex number displayed above plots).	11
2.4	The output of the optical hybrid plotted in phase space as Wigner functions with a coherent state Local Oscillator with $\alpha = 10$, and thermal state Input Signals at $\alpha = 5, 10, 15$	12
3.1	Comparison of photon number reconstruction results with the input coherent state.	16
3.2	Reconstruction comparison with thermal states, using units where $kT = \langle n \rangle$	17
3.3	Root mean squared error of the probability values between the reconstructed and original states. The error ratio is calculated by running the reconstructor for each average photon number, calculating the total RMSE, and dividing it by the mean value of the input distribution.	17
3.4	Simulated Z measurements using a signal with average photon number $\langle n \rangle = 5$ compiled into a histogram (simulated). [2]	18
3.5	Reconstructed photon number distribution (blue) and the original state (orange). . .	19
3.6	Ideal Coherent number state probabilities compared with the reconstructed state. The reconstructed state predicts an average photon number that is larger than the original number.	20

Listings

A.1	Strawberry Fields code for simulating the ideal optical hybrid.	23
B.1	Maximum Likelihood Estimator algorithm for reconstructing photon number statistics.	25
C.1	Plotting code for illustrating the outputs of the Strawberry Fields simulations in phase space using Wigner functions.	27

Index

90° optical hybrid, 3

ASE, 4

Colab notebook, 18

Decorator, 21

Error

Least Squares, 13

Fock basis, 8

Grating coupler, 2

homodyne detection, 5

jog, 9

KLayout, 4

local oscillator, 4

Mach-Zehnder interferometer, 3

Maximum likelihood estimator, MLE, 13

Phase Space, 8

Wigner function, 8

Photon number distribution, 13

Reconstruction, 13

Silicon photonics, 2

Strawberry Fields, 9

Transfer matrix, 5

Waveguide, 2

Y-branch, 3

Z measurement, 13